Jour. of the KGS, Vol. 18, No. 3. June 2002, pp. 73~85

# Cyclic Shear Strength of Anisotropically Consolidated Sand

## 비등방 압밀 모래의 반복 전단강도

Kim, Byung-Tak*1 김 병 탁 Kim, Young-Su*2 김 영 수
Seo, In-Shik*3 서 인 식 Jeong, Dong-Gil*4 정 동 길

### 요 지

본 논문에서는 비등방 압밀된 낙동강 포화모래의 비배수 반복 전단강도 거동이 연구되었으며, 등방압밀된 시료의 반복삼축시험은 비등방 압밀시료와의 비교를 위하여 수행되었다. 초기 정적 전단응력과 상대밀도의 다양한 조합하에 반복 전단강도는 고찰되었다. 응력반전과 비응력반전 모두에 대하여 반복하중을 받는 시료의 파괴는 5%의 양진폭변형율과 5%의 잔류축변형율로서 정의하였다. 비등방 압밀된 시료의 반복 전단강도는 초기 정적 전단강도에 영향을 받는 것으로 나타났다. 비등방 압밀 낙동강 모래의 반복 전단강도는 Toyoura 실리카 모래의 전단강도 보다는 크지만, Dogs Bay 카보나이트 모래의 전단강도 보다는 작게 나타났다. 실험결과와 예측결과의 비교에 의하면, 낙동강 모래의 잔류 간극수압에 대한 Hyodo 모델의 적용성이 입증되었다.

### Abstract

This paper is focused on studying the undrained cyclic triaxial behavior of saturated Nak-dong River sand, using anisotropically consolidated specimens. A test of isotropically consolidated specimens was performed to compare the results of the anisotropically consolidated specimens. The cyclic shear stre3ngth of the sand under various combinations of initial static shear stress and relative density was considered. Failure was defined as a 5% double amplitude cyclic strain and a 5% residual axial strain for both reversal stress and no reversal stress conditions. Using this definition, the cyclic strength of the anisotropically consolidated specimens was affected by the initial static shear stress. For anisotropically consolidated Nak-dong River dense sand, the cyclic strength is greater than that of Toyoura silica sand but is smaller than that of Dogs Bay carbonate sand. By comparing the experimental and predicted results, it was possible to predict the residual pore pressure of Nak-dong River sand using Hyodo's model with initial static shear stress subjected cyclic loading.

**Keywords** : Cyclic shear strength, Initial static shear stress, Liquefaction, Pore pressure, Sand, Triaxial test

## 1. Introduction

Liquefaction is one of the most important subjects in geotechnical earthquake engineering. Two major earthquakes - the Good Friday earthquake in Alaska and the Niigata earthquake in Japan - occurred in 1964. More recently, the Loma Prieta earthquake in 1989, the Kobe earthquake in 1995, and the Turkey earthquake in 1999 produced significant damage caused by liquefaction. Throughout the years, liquefaction associated with

*1 Member, Senior Researcher, Coastal & Harbor Engrg., Research Div., Korea Ocean Research & Development Institute (btkim@kordi.re.kr)
*2 Member, Professor, Dept. of Civil Engrg., Kyungpook National Univ.
*3 Member, Associate Professor, Dept. of Civil Engrg., Kyungdong College of Techno-Information
*4 Mass Transit & Railroads Dept., Seo Yeong Engrg. Co., LTD.

earthquake loading has been studied extensively around the world. South Korea is an area where liquefaction could potentionally occur. In 1987, the Hongsung earthquake, with a magnitude of 5.0, occurred.

The liquefaction or cyclic deformation potential of a level saturated sand deposit subjected to seismic or cyclic loads is commonly evaluated by undrained cyclic triaxial tests on isotropically consolidated specimens or cyclic simple shear tests on one-dimensionally consolidated specimens. In these tests, there is no initial static shear stress on horizontal planes prior to earthquake shaking. However, in practical ground conditions, soil elements inside soil structures such as soil slopes, earth dams and embankments or ground nearby structures are in a state of anisotropically consolidation. These structures are subjected to initial static shear stresses that are applied to the vertical/horizontal plane before being applied to the seismic loading. In an earth structure made of sand, the initial densities of the sand may be different from place to place. The effective confining pressures and stress ratios are also different from place to place. In other words, the initial states of the elements throughout the structure are in general different. When an earthquake occurs, some parts of the soil may contract while others may dilate. When a large deformation occurs after liquefaction is triggered, the structure configuration of the soil subjected to initial static shear stress may change differently from that of the soil subjected to an initial static shear stress of zero. As a result, the confining pressures may change accordingly. In addition, due to generation, redistribution and dissipation of excess pore pressures during an earthquake, the effective confining pressures will be characterized by additional changes. Therefore, the presence of these initial static shear stresses can have a major effect on the compressive characteristics and response of the soil to superimposed cyclic loading.

The present study focused on the effects of initial static shear stress on the subsequent cyclic shear behavior and strength without any rotation of principal stress axis. A series of undrained triaxial tests under various initial static shear stress conditions were performed to characterize the effect of stress reversal on the behavior of Nak-dong River sand. They include undrained monotonic triaxial compression tests and cyclic triaxial tests under isotropically /anisotropically consolidated sand. The results from a series of undrained cyclic triaxial tests on Nak-dong River sand were then compared with those of similar tests on Toyoura sand and Dogs Bay sand. The residual pore water pressure was predicted using Hyodo's model.

## 2. Previous Research Review

Lee and Seed (1967) simulated a ground condition where there was an initial static shear stress on the horizontal plane through the cyclic triaxial test for anisotropically consolidated specimens with an effective stress ratio of up to 1.0. The results of this study showed that the larger the initial static shear stress, the larger the resistance to liquefaction. On the other hand, the opposite tendency was presented by Yoshimi and Ohoka (1975) as a result of their ring torsional shear tests. They concluded that shear stress reversal was necessary to induce liquefaction or significant cyclic shear strain and that the resistance to liquefaction decreased with the increase of initial static shear stress. Ishihara and Takatsu (1977) performed torsional shear tests on medium dense sand. They concluded that an initial static shear stress increase induced an increase in resistance to the excess pore water pressure occurrence of the specimens.

Vaid and Finn (1978) and Vaid and Chern (1983) showed that the contradictory conclusions in past studies were due to differences in the relative density of the samples, the magnitudes of the initial static shear stress and the definition of resistance to liquefaction. In addition, they concluded that cyclic strength could either increase or decrease due to the presence of an initial static shear stress. Hasegawa *et al.* (1982) performed undrained cyclic triaxial tests on anisotropically consolidated volcanic sands and defined cyclic failure as the time when the rate of axial strain development becomes constant. They divided the behavior of samples subjected to various initial static and subsequent cyclic shear stresses into three region types: failed, transient and stable. Uchida and Hasegawa (1986) further showed that the dynamic

failure criterion of soil subjected to an initial shear stress could be defined by a specified permanent strain of 10% for the testing volcanic sands.

Hyodo *et al.* (1991) performed an undrained cyclic triaxial test with two relative densities of 70% and 50% to classify the cyclic failure pattern, quantify the pore pressure and residual shear strain, and develop a model to evaluate the pore pressure and residual strain. Based on the results of their laboratory program, they found that the cyclic failure pattern of saturated sand with an initial static shear stress was classified by the relative magnitude correlation of initial static and cyclic shear stresses. In addition, it was recognized that there is a unique relationship between the cyclic shear strength ratio and relative effective stress ratio, in other words, the relative situation between the initial and failure states in the *p-q* diagram. Hyodo *et al.* (1996) performed a series of drained and undrained monotonic triaxial tests together with a series of drained cyclic triaxial tests on crushable carbonate sand in Dogs Bay. The results were compared with similar tests on a less crushable standard silica sand. They concluded that the cyclic strength of carbonate sand increased with the increase of initial static shear stress. However, the rate of increase was less than that of Toyoura sand. Additionally, they found that the normalized cyclic strength of specimens anisotropically consolidated with an initial static shear stress was dependent on the initial confining pressure.

## 3. Experimental Procedures

### 3.1 Soil Tested

The Nak-dong River sand used in these tests contained sub-angular and sand particles with up to 80% quartz content. Fig. 1 shows the scanning electron micrograph (SEM) of the Nak-dong River sand particles. The sand was obtained from a beach deposit in Hwawon, a city located west of Daegu. The particle size distribution for the Nak-dong River sand as well as Toyoura sand and Dogs Bay sand is shown in Fig. 2. Table 1 gives the physical properties for each sand. When the specimens were prepared using the dry method (Yamamuro and Lade, 1997) the maximum and minimum void ratios were established according to ASTM standards 4253 and 4254 (dry methods). The Nak-dong River sand has the highest $D_{50}$ and has an intermediate specific gravity, along with

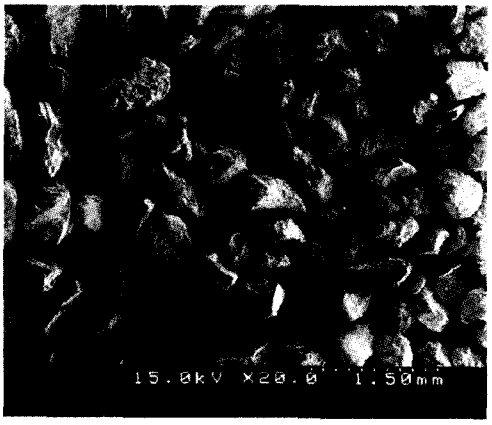


Fig. 1. SEM of Nak-dong River sand

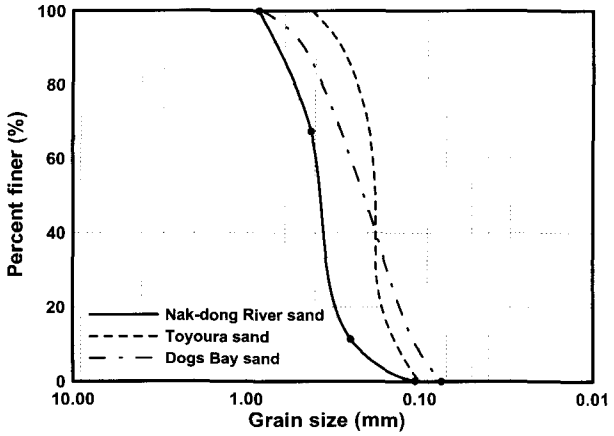


Fig. 2. Grain size distribution of samples

Table 1. Physical properties of Dogs Bay sand, Toyoura sand and Nak-dong River sand

| Sands | $G_s$ | $D_{50}$ | $U_c$ | $e_{max}$ | $e_{min}$ | Roundness |
|---|---|---|---|---|---|---|
| Nak-dong River sand | 2.676 | 0.36 | 1.23 | 1.137 | 0.765 | Subangular |
| Toyoura sand | 2.643 | 0.18 | 1.20 | 0.973 | 0.635 | Subangular |
| Dogs Bay sand | 2.723 | 0.21 | 1.92 | 2.451 | 1.621 | Highly angular |

maximum and minimum void ratios. The Nak-Dong River sand used in these tests was clean, having been washed with flowing water and sieved to #20~#200.

### 3.2 Equipment

To perform the stress-controlled cyclic triaxial tests, the Automated Triaxial Testing System, located at Kyungpook National University in Daegu and developed by C. K. Chan, was used (Li, 1988). Loading was controlled by a closed-loop feedback scheme capable of performing stress or strain controlled tests in the standard triaxial environment. The system has two control channels, allowing separate control of both the axial load and the chamber pressure. Loading conditions were microprocessor controlled and electronic instrumentation was used for data acquisition and processing.

### 3.3 Specimen Preparation

The specimen preparation method used for all specimens is the dry funnel deposition method. This method was performed by placing dry sand into a funnel with a small tube attached to the spout. The tube was placed at the bottom of the specimen split-mould. The tube was also slightly raised from the bottom of the cylindrical mould in such a way that the sand was deposited without any drop height. This provided the loosest possible density. Denser specimens were achieved by gently tapping on the split-mould in a symmetrical pattern, in order to achieve a more uniform density and the required specimen height. All the specimens were basically prepared by tapping the split-mould with a 20 mm diameter tamping rod. The diameter of the prepared specimen was measured after a 10 kPa vacuum was applied and the split-mould was removed keeping the vacuum. Both the diameter and height of the specimen were measured to the nearest 0.05 mm. The specimen diameter was determined at three locations - the top, bottom and middle - and the average value was used for density calculations. Final specimen dimensions were 140 mm in height and 70 mm in diameter. Triaxial membrane thickness was subtracted from the diameter to calculate the void ratio.

### 3.4 Testing Procedure

Cyclic triaxial tests were carried out using the following procedures under initial isotropic and anisotropic consolidation conditions and constant value of a 100 kPa mean normal effective consolidation stress $p_c'=(\sigma_{1c}' + 2\sigma_{3c}')/3$.

First, to achieve fully saturated specimens in a reasonable amount of time, a saturation procedure called the 'vacuum' procedure was used. To obtain reliable pore pressure change measurements and prevent volume changes during undrained loading, it was necessary to

Table 2. Summary of cyclic triaxial tests in the present study

| Density | $q_s$ (kPa) | $q_{cyc}$ (kPa) | $P_c'$ (kPa) | $\sigma_{1c}'$ (kPa) | $\sigma_{3c}'$ (kPa) | $K_c$ | Stress reversal |
|---|---|---|---|---|---|---|---|
| Loose | 0 | 27, 30, 35, 40, 44 | 100 | 100 | 100 | 1.0 | R* |
| | 20 | 30, 35, 40, 43, 45 | 100 | 113.3 | 93.3 | 1.21 | R |
| | 40 | 27, 30, 35, 40, 48 | 100 | 126.7 | 86.7 | 1.46 | R or N** |
| | 60 | 25, 30, 35, 38, 50 | 100 | 140 | 80 | 1.75 | N |
| | 80 | 25, 30, 35, 40 | 100 | 153.3 | 73.3 | 2.09 | N |
| Dense | 0 | 40, 45, 50 | 100 | 100 | 100 | 1.0 | R |
| | 20 | 50, 55, 62 | 100 | 113.3 | 93.3 | 1.21 | R |
| | 40 | 55, 60, 68 | 100 | 126.7 | 86.7 | 1.46 | R |
| | 60 | 70, 80, 85 | 100 | 140 | 80 | 1.75 | R |
| | 80 | 85, 90, 95, 100 | 100 | 153.3 | 73.3 | 2.09 | R or I*** |

* : Reversal stress condition
** : No-reversal stress condition
*** : Intermediate stress condition

achieve saturation prior to loading. When a Skempton's B-value larger than 0.95 was reached, the specimens were accepted as fully saturated for this research. Saturation was completed with the help of a 200~250 kPa back pressure. During saturation, no changes in specimen dimensions occurred. Effective consolidation pressures ( $\sigma_{3c}'$) were then increased to their final values of 73.3, 80, 86.7, 93.3 and 100 kPa with the backpressure. For the isotropically cyclic tests, an initial effective consolidation pressure of 100 kPa was applied. For the anisotropically cyclic tests, an initial effective consolidation pressure of 73.3~93.3 kPa was applied. In the case of the anisotropically cyclic tests, an initial deviator stress $q_s$ for both loose and dense sand was applied at 20, 40, 60 and 80 kPa during the consolidation period. The initial relative density of specimens before consolidation was estimated to be 34% (loose) and 77% (dense). The conditions of the triaxial cyclic tests are summarized in Table 2.

Monotonic undrained tests were also performed on the specimens with the same relative densities and mean normal effective consolidation stresses of $p_c'$ = 100, 200 and 300 kPa at an axial deformation of 0.1%/min using the same triaxial apparatus. These tests were carried out in order to determine the failure envelope. Cyclic triaxial tests were performed with the sinusoidally cycled deviator stress at a frequency of 0.1 Hz under undrained conditions and constant effective consolidation pressure. Cyclic loading was used for stress control type. About three to five magnitudes of cyclic deviator stress ($q_{cyc}$) were combined with each static deviator stress so that both reversal and no-reversal cyclic shear stresses were simulated. In order to portray the stress reversal conditions, the terms 'reversal', 'no-reversal' and 'intermediate' are used in the present study, based on the ratio of cyclic deviator stress to initial static shear stress, $q_{cyc}/q_s$. During these tests, axial stress, axial displacement and pore water pressure data were automatically monitored and stored by a computer.

## 4. Test Results

### 4.1 Monotonic Shear Tests

Undrained monotonic shear tests were performed on the Nak-dong River sand. The effective stress paths of undrained compression and extension tests as well as the associated stress strain curves for loose clean Nak-dong River sand are shown in Fig. 3.

In this figure, the phase transformation lines for both the compression and extension states are clearly evident. In addition, the effective stress ratio ($q/p'$) at the phase transformation point is independent of the mean normal effective consolidation stress ($p_c'$). The slope of the phase transformation line (PTL) is equal to 1.3 for the compression state and 0.85 on the extension state. These lines are drawn as continuous through the origin and can be

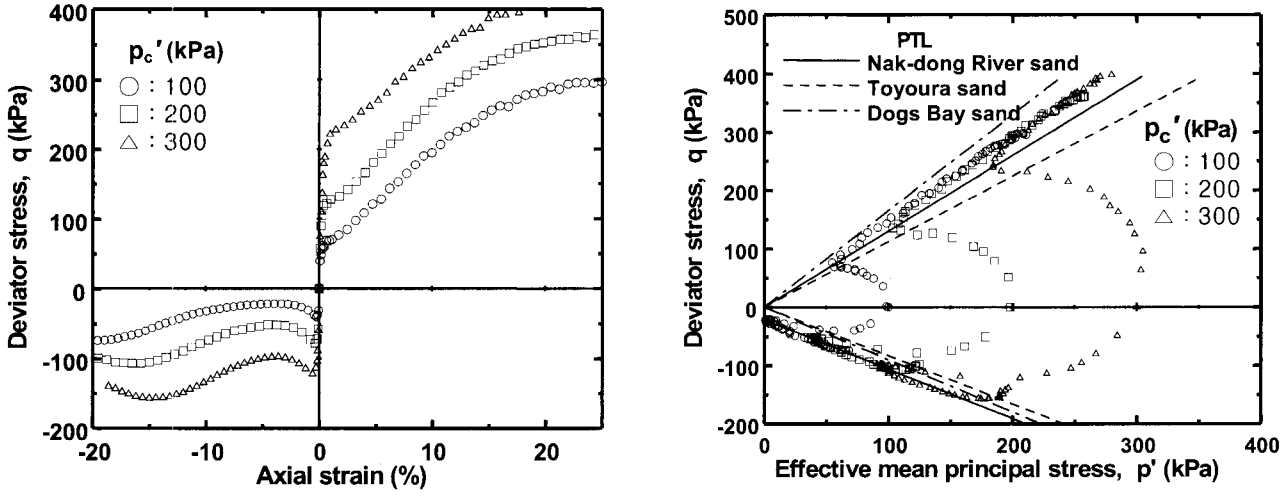


Fig. 3. Undrained shear behavior of Nak-dong River sand under compression and tension loading

compared with the dotted lines used for the phase transformation of the Toyoura and Dogs Bay sands, whose slopes were 1.12 (Toyoura sand) and 1.65 (Dogs Bay sand) in compression and 0.83 (Toyoura sand) and 0.90 (Dogs Bay sand) in extension. The PTL slope for loose clean Nak-dong River sand was closer to the values of the Toyoura sand. This indicates that the Nak-dong River sand is characteristically anisotropic like the Toyoura and Dogs Bay sand. However, the undrained stress strain curves demonstrate much more brittle behavior under undrained conditions, with sample strengths reaching a definite initial peak before the strength increased more gently at much higher strains.

### 4.2 Cyclic Shear Tests

Hyodo *et al.* (1991) classified cyclic failure patterns in three ways. Fist, if the value of $q_{cyc}/q_s$ is larger than 1.0, the cyclic failure is in a state of 'Reversal'. Second, if $q_{cyc}/q_s$ is smaller than 1.0, the cyclic failure is in a state of 'No-reversal' because there is no stress reversal. Finally, if $q_{cyc}/q_s$ is between 0.9 and 1.1, the cyclic failure is in the 'Intermediate' state.

The typical effective stress paths during cyclic loading for loose ($D_r$=34%) and dense ($D_r$=77%) clean Nak-dong River sand in each loading pattern are shown in Figs. 4 and 5, respectively. The failure envelope lines and phase transformation lines obtained from the monotonic loading tests are also drawn in these figures. For the dense sand, the effective stress paths shown on the loading pattern are reversal and intermediate cases because the effective stress path for no-reversal remained unchanged due to the lack of developing axial strain. Based on Fig. 4, it was found that the cyclic shear behavior differed greatly, depending on the initial static shear stress, despite the fact that a similar cyclic shear stress was applied.

In the reversal case, with $q_{cyc}/q_s = \propto$ (Figs. 4a, 5a and 5b), the effective stress path moved toward the failure envelope due to an increase in pore water pressure during cyclic loading. Additionally, the cyclic failure occurred suddenly after crossing the failure envelope line of the extension state. For the dense sand, however, the effective stress path exhibited typical cyclic mobility behavior, repeating the failure envelope from compression to extension. It slowly moved toward the failure envelope and finally traced a steady loop, slightly crossing the failure envelope. While the effective stress path of the specimen with $q_s$ = 0.0 moved rapidly toward the failure envelope, that of the specimen with $q_s$ = 40 kPa slowly moved toward the envelope. This was due to the effect of the initial static shear stress. It also required a greater number of cycles.

In the intermediate case, with $q_{cyc}/q_s$ = 0.88 ~ 1.06 (Figs. 4b and 5c), the effective stress path moved slowly toward the failure envelope until the upper end of the stress path touched it. In addition, liquefaction occurs in neither the loose nor dense sand. The cyclic strain amplitude in the loose sand greatly developed, but that of the dense sand remained relatively small. Nonetheless, a gradual accumulation of residual strain was observed in the dense sand. If the axial strain at failure assumed 8% ultimately, it sometimes brought the specimens to failure even though no liquefaction occurred.

In the no-reversal case, with $q_{cyc}/q_s$ = 0.44 (Fig. 4c), the effective stress path rapidly moved toward the failure envelope due to a sudden increase in pore water pressure compared to the reversal and intermediate cases. A residual strain for both the loose and dense sand occurred continuously, but the increase rate of the pore water pressure remained constant.

By comparing the effective stress paths and stress-strain relationships, it is recognized in general that significant cyclic strain amplitude develops when the effective stress path is tangential with the failure envelope. In addition, a significant amount of residual strain accumulates when the specimen was dense sand in the reversal case.

The effects of initial static shear stress ($q_s$) on the relationship between pore water pressure and number of cycles for loose and dense clean Nak-dong River sands are shown in Fig. 6. In the present study, the axial strain for isotropically consolidated specimens is a double amplitude strain (*DA*). For anisotropically consolidated specimens, it is a residual strain (*RA*).

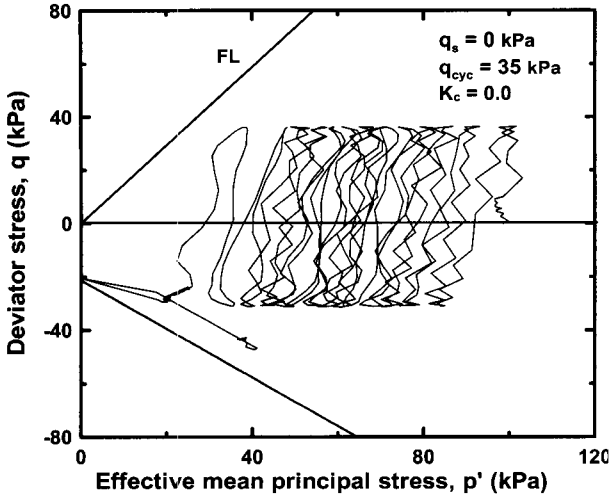


(a) Reversal ($q_{cyc}$ / $q_s$ = $\infty$)

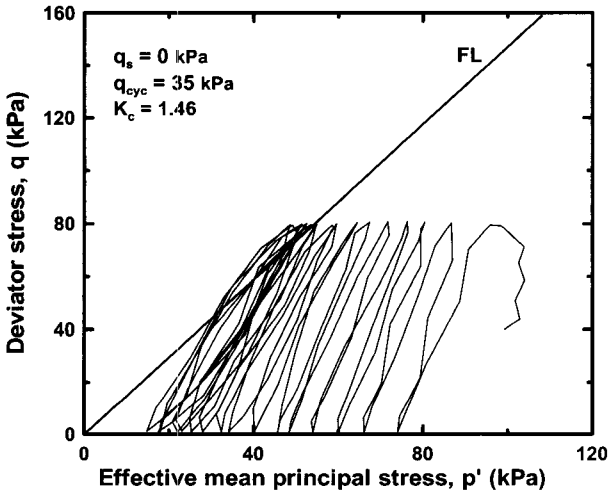


(b) Intermediate ($q_{cyc}$ / $q_s$ = 0.88)

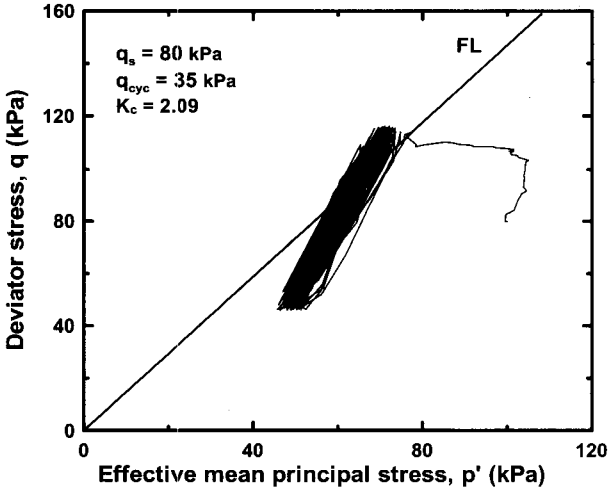


(c) No-reversal ($q_{cyc}$ / $q_s$ = 0.44)

Fig. 4. Effective shear stress path for each cyclic stress pattern in loose sand

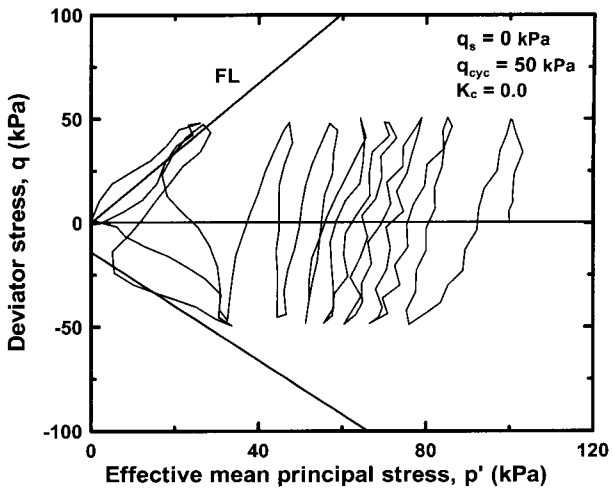


(a) Reversal ($q_{cyc}$ / $q_s$ = $\infty$)

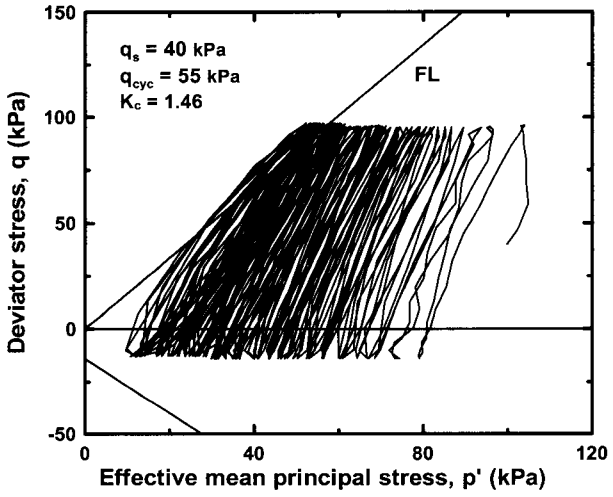


(b) Reversal ($q_{cyc}$ / $q_s$ = 1.38)

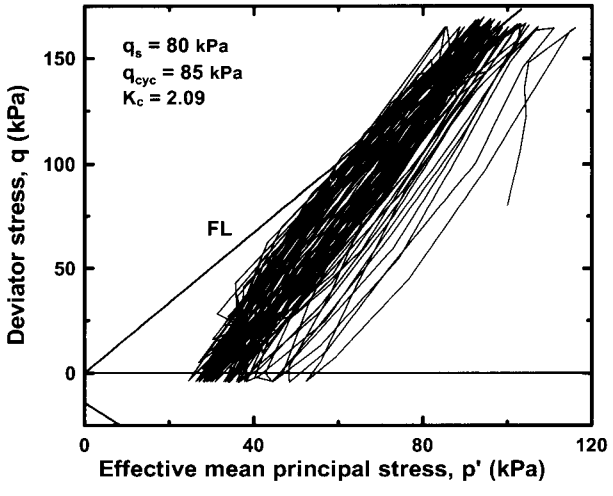


(c) Intermediate ($q_{cyc}$ / $q_s$ = 1.06)

Fig. 5. Effective shear stress path for each cyclic stress pattern in dense sand

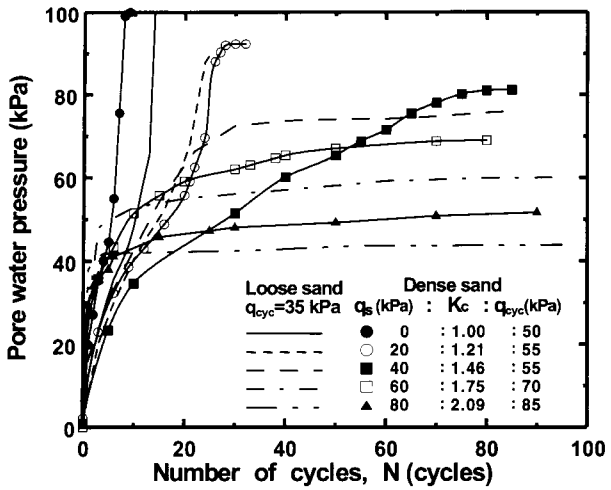


Fig. 6. Effect of initial static shear stress on pore water pressure -*N* relationship under loose and dense sands

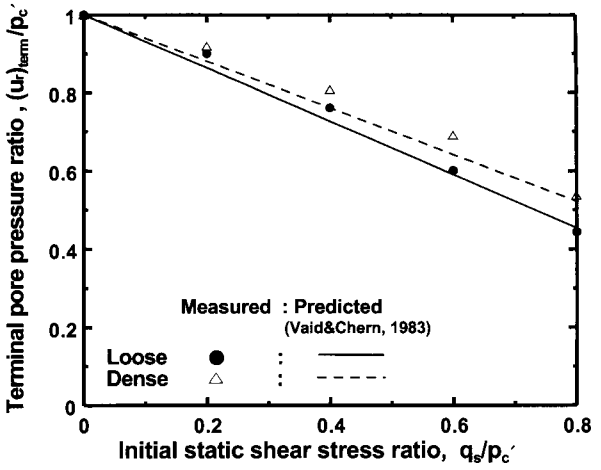


Fig. 7. Relationship between the terminal residual pore water pressure and initial static shear stress ratio

Although the loose sand specimens had the same 35 kPa cyclic shear stress $q_{cyc}$ applied for each stress reversal condition, the behaviors of the axial strain and pore water pressure with an increasing number of cycles clearly depended on the magnitude of the initial static shear stress. These tendencies were similar to the dense sand specimens. In the reversal case, the pore water pressure continuously increased with an increasing number of cycles, but becomes constant at a large number of cycles. Both the loose and dense sand specimens may fail as well due to the rapid increase in axial strain. In the no-reversal case, however, the pore water pressure becomes constant after a rapid increase in pore water pressure at a smaller number of cycles. In addition, the failure of both loose and dense sand occurred at this stage because of the excess development of residual strain rather than liquefaction.

Fig. 6 shows that the terminal value of residual pore water pressure decreases with the increase of consolidation stress ratio ($K_c$) or initial static shear stress. However, it is independent of the relative density of the specimen and cyclic shear stress amplitude applied. Such tendencies are also recognized in the results of Vaid and Chern (1983). To review the application of the theoretical function suggested by Vaid and Chern (1983), the Nak-dong River sand experimental results of the relationship between the terminal residual pore water pressure and initial static shear stress ratio were compared with the theoretical results. The comparison results are shown in Fig. 7. The angle of internal friction ( $\phi'$) was obtained from the monotonic undrained triaxial test. It was also found that there is a reasonably high degree of correlation between our experimental results and the theoretical results of Vaid and Chern (1983).

## 4.3 Cyclic Shear Strength

Undrained cyclic strength characteristics of saturated sand with an initial static shear stress depend on the relative density, confined stress and soil structure. In addition, the definition of cyclic shear strength plays a very important role in the undrained cyclic strength characteristics. The definition of cyclic shear strength is the magnitude of strain at the soil failure state caused by cyclic shear stress. In the reversal case, generally, the strain is a double amplitude (*DA*) of 5% and initial liquefaction occurs at *DA* = 5%. In the no-reversal case, because of specimen failure occurs through the excess development of residual strain, the strain is defined differently, following a residual strain (*RS*) of 5% by Mohamad and Dobry (1986) and *RS* = 10% by Uchida and Hasegawa (1986). In this study, failure was therefore defined by a 5% residual strain limit for both the reversal and no-reversal cases, as well as defined by a 5% double amplitude limit for the loose sand.

The cyclic shear strength of clean Nak-dong River

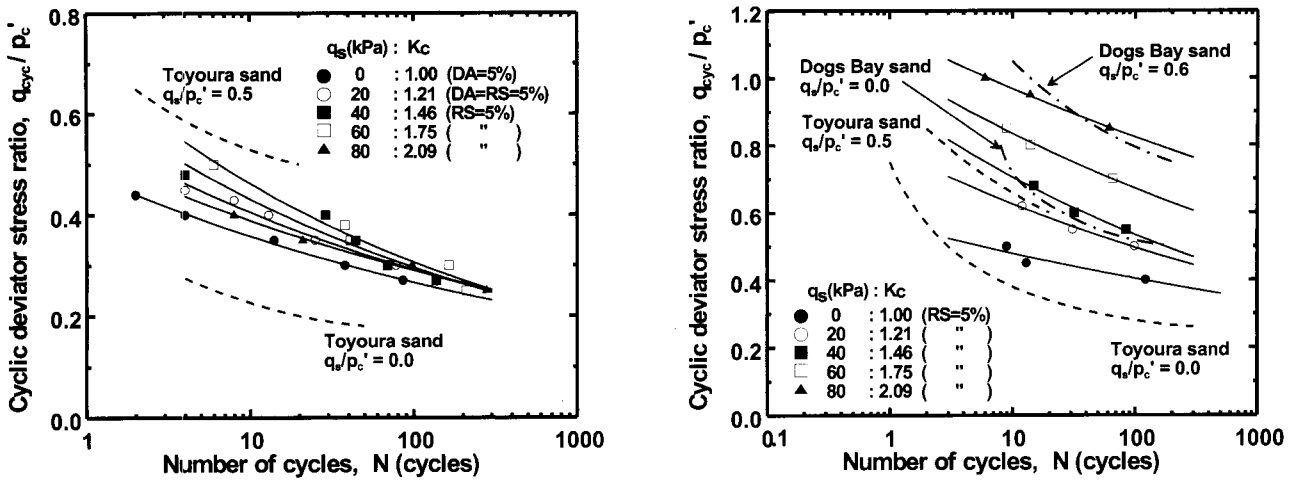


(a) Loose sand (b) Dense sand

Fig. 8. Relationship between cyclic deviator stress ratio and number of cycles to cause DA or RS = 5% under anisotropically consolidated condition

sand was investigated at various initial static shear stresses. Although the initial relative density ($D_r$ = 34% and 77%) before consolidation was identical for all specimens, it increased with an increasing confining stress up to 40% for loose sand and up to 80% for the dense sand. The relationship between the cyclic deviator stress ratio ($q_{cyc}/p_c'$) and number of cycles to cause *DA* or *RS* equal to 5% for isotropically and anisotropically consolidated undrained cyclic tests is shown in Fig. 8. In this figure, the curves for Toyoura sand with $D_r$ = 50 and 70% and Dogs Bay sand with $D_r$ = 80% can also be seen. As can be seen for the loose sand, the cyclic shear strength increased with the level of initial static shear stress until the initial static shear stress ratio $q_s/p_c'$ = 0.6. However, the strength decreased remarkably under $q_s/p_c'$ = 0.8. The reason for this may be that under a significant level of initial static shear stress, a significant flow deformation at the compression state occurred during the initial cyclic loading since the maximum deviator stress (= $q_s$ + $q_{cyc}$) was larger than the shear strength ($S_{PT}$) at the point of phase transformation.

For the dense sand, however, phenomena such as flow deformation didn't occur. Then, however, a cyclic shear strength that caused *RS* = 5% increased with the level of initial static shear stress until the initial static shear stress ratio $q_s/p_c'$ = 0.8. The cyclic shear strength for the Nak-dong River sand, with $D_r$ = 34%, can be considered to be relatively narrow range compared to the data for Toyoura sand ($D_r$ = 50%) of $q_s/p_c'$ = 0.0~0.5 as the number of cycle increased. The cyclic shear strength for Nak-dong River sand, with $D_r$ = 77%, also can be considered to be relatively wide range compared to the data for Toyoura sand ($D_r$ = 70%) of $q_s/p_c'$ = 0.0~0.5 and Dogs Bay sand ($D_r$ = 80%) of $q_s/p_c'$ = 0.0~0.6 as the number of cycle increases.

Fig. 9 shows the relationship between the cyclic deviator stress ratio and initial shear stress ratio, which caused *DA* and *RS* equal to 5% in 10 cycles. The results for Toyoura sand with $D_r$ = 40% and Dogs Bay sand with $D_r$ = 80% are also shown. It is found from the figure that while for dense sand, a cyclic stress reversal is necessary to accumulate a damaging level of residual strain, for loose sand, a significant amount of residual strain also develops under the no-reversal stress condition. It is found from Fig. 9a that although the cyclic deviator stress ratio increased with an increasing initial static shear stress until $q_s/p_c'$ = 0.6, the cyclic deviator stress ratio at $q_s/p_c'$ = 0.8 in a residual strain of 5% is smaller than that at $q_s/p_c'$ = 0.2. The tendency in a residual strain of 8% is similar to that of a residual strain of 5%. However, the cyclic deviator stress ratio at $q_s/p_c'$ = 0.8 is larger than that at $q_s/p_c'$ = 0.2 and 0.4. These results indicate that the definition of failure criteria for cyclic shear strength affects the characteristics of cyclic shear

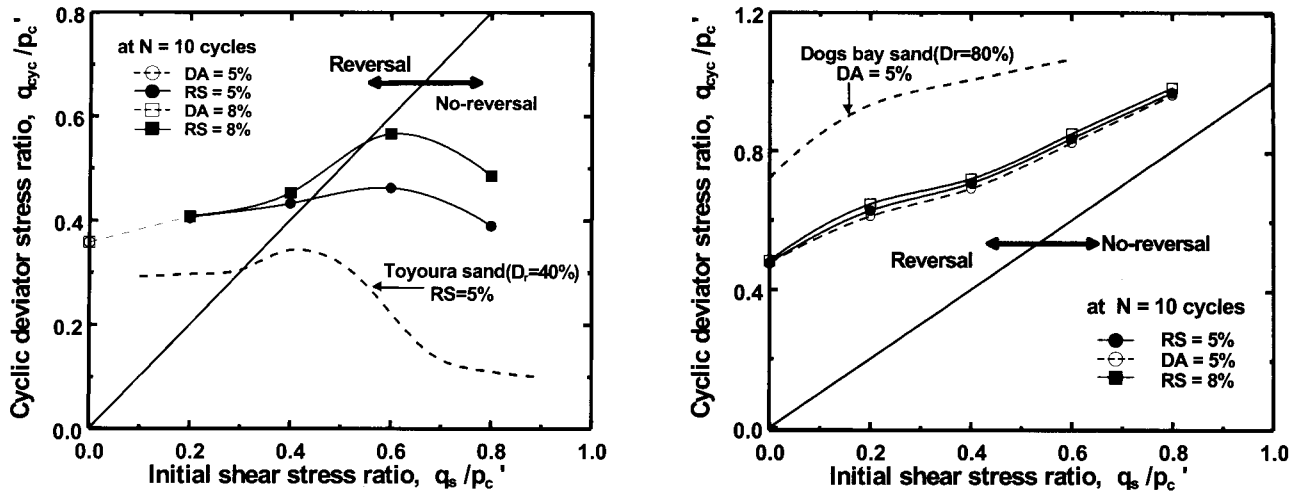


(a) Loose sand

(b) Dense sand

Fig. 9. Relationship between the cyclic deviator stress ratio and initial static shear stress ratio to cause RS=5% and 8% in 10 cycles

Table 3. Comparison with Toyoura sand and Nak-dong River sand for the values of $\beta$ and $\kappa$

| Sand | Relative density | $\beta$ | $\kappa$ |
|---|---|---|---|
| Toyoura sand | 70% | −0.115 | 0.470 + 0.737 $q_s$ / $p_c'$ |
| | 50% | −0.115 | 0.297 + 0.804 $q_s$ / $p_c'$ |
| Nak-dong River sand | 77% | −0.162 | 0.688 + 0.574 $q_s$ / $p_c'$ |
| | 34% | −0.106 | 0.487 + 0.355 $q_s$ / $p_c'$ |

strength. In the case of dense sand (Fig. 9b), however, the cyclic deviator stress required to cause *RS* = 5% and 8%, respectively, increased with an increasing initial static shear stress on the reversed shear stress side. In addition, by comparing the results of the Nak-dong River and Dogs Bay sand for dense sand, the cyclic shear strength for Dogs Bay sand is greater than that of the Nak-dong River sand. However, the increase rate of the cyclic strength for the Nak-dong River sand is greater than that for the Dogs Bay sand as the initial static shear stress increases. This is thought to be due to the angularity and crushability of the skeletal particles. In the loose sand, by comparing the results of the Nak-dong River and Toyoura sand for dense sand, the decrease in cyclic shear strength for the Toyoura sand under the no-reversal stress condition is similar to that of the Nak-dong River sand. However, the magnitude of the cyclic strength for the Toyoura sand is less than that for the Nak-dong River sand.

Hyodo *et al.* (1991) has proposed the experimental function on the relationship between the cyclic deviator stress ratio ($q_{cyc}/p_c'$) and number of cycles ($N$) for the Toyoura sand. This function is given by parallel straight lines for each initial static shear stress ($q_s$) and then formulated as follows:

$$R_f=(q_{cyc}/p_c')_f=\kappa N^{\beta} \quad (1)$$

where, $\beta$ is the slope of the lines and $\kappa$ is the intercept of each line with $N$ = 1.

The parameters of $\beta$ and $\kappa$ for the Nak-dong River sand compared with the values for the Toyoura sand and are shown in Table 3. Equation (1) was used to predict the pore water pressure and residual axial strain.

## 5. Results from the Comparison with Hyodo's Model

### 5.1 Determination of the Relationship Between $\eta^*$ and $R/R_f$

The relationship between the relative effective stress

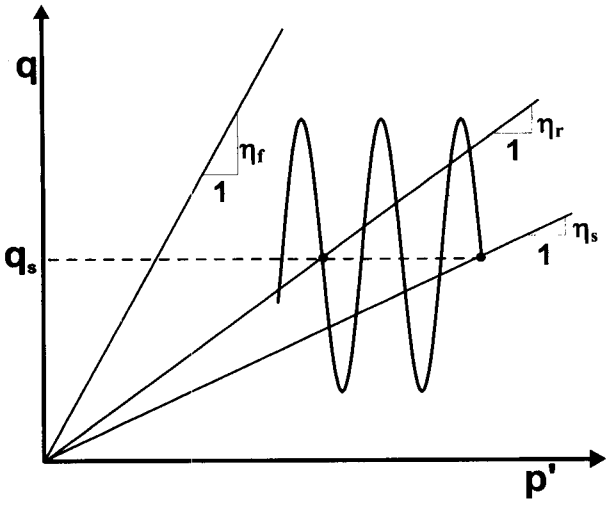


Fig. 10. Concept of relative effective stress ratio during undrained cyclic loading (Hyodo et al., 1991)

ratio ( $\eta^*$) and cyclic shear strength ratio ($R/R_f$) is defined by Hyodo *et al.* (1991). They mentioned that when a cyclic load with a uniform amplitude ($R$) in a given initial static shear stress is applied, the cyclic strength ($R_f$) corresponding to the initial static shear stress and the number of cycles is selected and the ratio $R/R_f$ is evaluated. The relative effective stress ratio is also defined by Hyodo *et al.* (1991) and formulated as follows:

$$\eta^* = (\eta_r - \eta_s)/(\eta_f - \eta_s) \tag{2}$$

where, $\eta_r$ is the effective stress ratio at the end of a given number of cycles, $\eta_s$ is the effective stress ratio of the initially anisotropically consolidated condition and $\eta_f$ is the effective stress ratio at failure. A $p'$ - $q$ diagram for each situation is shown in Fig. 10. It may be noted in the figure that the relative effective stress ratio represents the state of degradation during cyclic loading in terms of the initial and failure possible states of the effective stress ratio in a $p'$ - $q$ diagram. Thus, when $\eta^*$ = 0, the soil is in the initial consolidated condition and when $\eta^*$ = 1.0, the soil is at failure due to cyclic loading.

Fig. 11 shows the relationship between $\eta^*$ and $R/R_f$ for loose and dense Nak-dong River sand. It can be seen from the figure that a unique relationship exists between $\eta^*$ and $R/R_f$ under the same initial static shear stress conditions. It is also found that although these relationships depend on the initial static shear stress, they are independent of the magnitude of applied cyclic shear stresses. Based on these relationships, the relative effective stress ratio ( $\eta^*$) can be formulated again as follows (Hyodo *et al.*, 1991):

$$\eta^* = \frac{(R/R_f)}{a-(a-1)\cdot(R/R_f)} \tag{3}$$

where, $a$ is an experimental parameter related with the initial static shear stress ratio for each density of sand. The parameters $a$, under the condition of $0 < q_s/p_c' < 0.8$, are a = 0.719 $q_s/p_c'^{-2.83}$ for loose sand and $a$ = 2.288

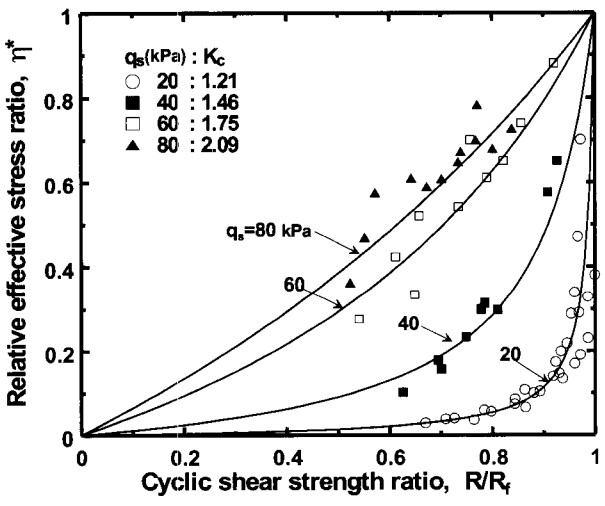


(a) Loose sand

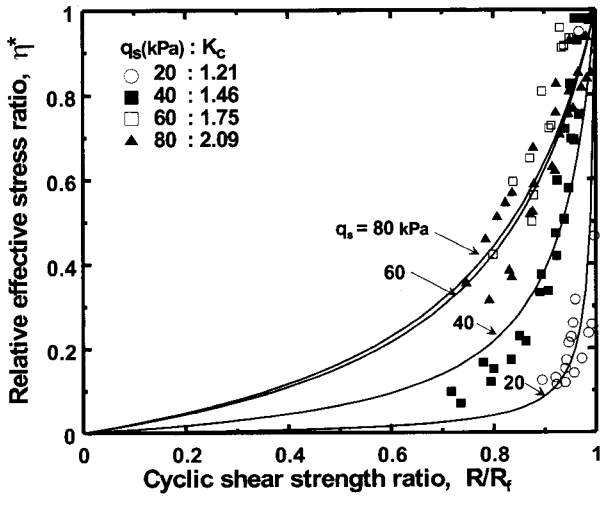


(b) Dense sand

Fig. 11. Relationship between relative effective stress ratio and cyclic shear strength ratio

$q_s/p_c'^{-2.29}$ for dense sand. The determination coefficients of the experimental functions obtained are more than 0.96.

## 5.2 Prediction of Pore Water Pressure

The above experimental findings were used to predict the residual pore water pressure ($u_r$) and residual axial strain ($\varepsilon_r$) in each stress cycle. A simplified method to predict them was suggested by Hyodo *et al.* (1991). This method was thus used in this research. The method uses the relationship between the cyclic deviator stress ratio ($q_{cyc}/p_c'$) and number of cycles ($N$), as well as the relationship between relative effective stress ratio ($\eta^*$) and cyclic shear strength ratio ($R/R_f$). Using these relationships, the residual pore water pressure in each stress cycle with a given initial static shear and cyclic shear stress was predicted. In addition, the calculation procedure of the method employed to predict these values is described in detail by Hyodo *et al.* (1991). As a result, in this paper, a detailed procedure was omitted. Instead, the final equation for the residual pore water pressure is as follows:

$$U_r = p_c' - q_s/\eta_r \quad (4)$$

where, $\eta_r$ is the effective stress ratio at the end of a given number of cycles. The parameter $\eta_r$ can be determined by the equation of $\eta_r = \eta^*(\eta_f - \eta_s) + \eta_s$, where $\eta^*$ is determined by Eq. (3) and $\eta_f$ and $\eta_s$ are the constant values for each cyclic triaxial test.

The predicted and observed residual pore pressures for the dense and loose sand are shown in Fig. 12. In this figure, the predicted and observed results correspond to the plots and solid lines, respectively. By comparing them, it can be recognized that there is good agreement between the predicted and observed results, especially in both the initial number of cycles and reversal stress condition. Incidentally, the results were not related to the relative density of sand. For Nak-dong River loose sand, it was found that there is a lack of good agreement between the predicted and observed results, especially in the initial number of cycles due to the occurrence of flow deformation. However, the predicted results at a certain number of cycles near the occurrence of liquefaction are comparatively close to the observed results. For Nak-dong River dense sand, it was found that there is good agreement between the predicted and observed results, especially with a high initial static shear stress compared to the results for loose sand.

The difference between the predicted and experimental results is shown in Fig. 12. It is mainly due to the scatter of plots in determining the parameters of $\kappa$, $\beta$, and $a$. However, it is confirmed by this verification that Hyodo's model is reasonable in predicting residual pore pressure

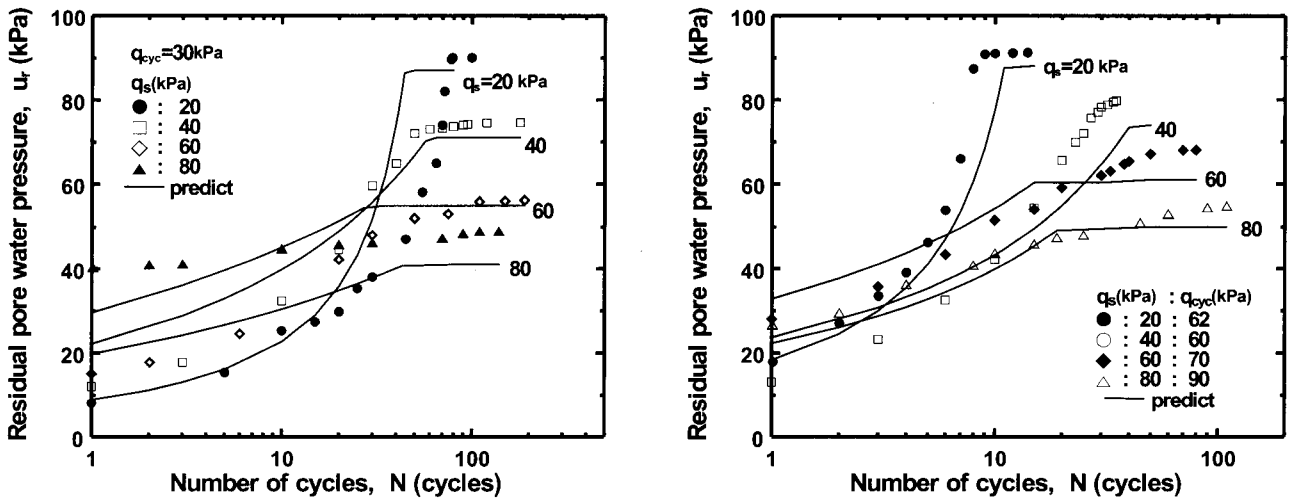


(a) Loose sand (b) Dense sand

Fig. 12. Comparison of predicted and observed residual pore pressure with various initial static shear stress

of saturated Nak-dong River sand subjected to initial static shear stress and subsequent cyclic shear stresses.

## 6. Conclusions

Cyclic triaxial tests were performed on the Nak-dong River sand. The following conclusions can be drawn from the tests:

(1) Liquefaction failure for loose sand occurred due to cyclic mobility in the reversal stress condition. However, it was due to the residual axial strain in the no reversal stress condition. Liquefaction failure for dense sand occurred in only the stress reversal condition.

(2) For both dense and loose sand, the behaviors of the axial strain and pore water pressure with an increasing number of cycles clearly depended on the magnitude of the initial static shear stress.

(3) The normalized cyclic shear strength as the number of cycle increased, to cause 5% of double amplitude of axial strain and residual axial strain, increased with the increase of initial static shear stress. The cyclic shear strength as initial static shear stress increased for Nak-dong River dense sand can be considered relatively wide compared to the data for the Toyoura sand and Dogs Bay sand.

(4) The cyclic shear strength of Nak-dong River dense sand, to cause a 5% residual axial strain, increased with an increasing initial static shear stress on the reversal stress side. However, the rate of increase is greater than that of the Dogs Bay sand.

(5) By comparing the experimental and predicted results, it was confirmed that Hyodo's model is reasonable in predicting residual pore pressure of saturated Nak-dong River sand subjected to an initial static shear stress and subsequent cyclic shear stresses.

## References


1. ASTM, Standard Test Method for Load Controlled Cyclic Triaxial Strength of Soil, *D5311, USA.*
2. Hasegawa, T., Uchida, K. and Tateishi, T. (1981), "Dynamic critical line of a soil subjected to initial shear stress", *17th Japan National Conf. on Soil Mech. and Found. Engrg.*, Naha, Okinawa, pp.1589-1592 (in Japanese).
3. Hyodo, M., Murata, H., Yasufuku, N., and Fujii, T. (1991), "Undrained cyclic shear strength and resisual shear strain of saturated sand by cyclic triaxial tests", *Soils and Foundations*, Vol.31, No.3, pp.60-76.
4. Hyodo, M., Aramaki, N., Itoh, M., and Hyde, A. F. L. (1996), "Cyclic strength and deformation of crushable carbonate sand", *Soil Dynamics and Earthquake Engineering*, Vol.15, No.5, pp. 331-336.
5. Ishihara, K. (1980), "Current practice and problems in the earthquake resistant design of earth structures", *JSSMFE*, Vol.8, No.8, pp.3-8 (in Japanese).
6. Lee, K. L. and Seed, H, B. (1967), "Dynamic strength of anisotropically consolidated sand", *Journal of Geotechnical Engineering Division, ASCE*, Vol.93, No.SM5, pp.169-190.
7. Li, X. S. (1988), "An automated triaxial testing system", *Advanced Triaxial Testing of Soil and Rock*, ASTM STP 966, eds. R. T. Donaghe, R. C. Chaney & M. L. Silver, ASTM, Philadelphia, pp.95-106.
8. Mohamad, R., and Dobry R. (1986), "Undrained monotonic and cyclic triaxial strength of sand", *Journal of Geotechnical Engineering Division, ASCE*, Vol.112, No.10, pp.941-958.
9. Uchida, K. and Hasegawa, T. (1986), "Strength - deformation characteristics of a soil subjected to initial shear stress", *Soils and Foundations*, Vol.26, No.1, pp.11-24.
10. Vaid, Y. P. and Chern, J. C. (1983), "Effects of Static Shear on Resistance to Liquefaction", *Soils and Foundations*, Vol.23, No.1, pp.47-60.
11. Vaid, Y. P. and Finn, W. D. L. (1978), "Static shear and liquefaction potential", *Journal of Soil Mechanics and Foundation Division, ASCE*, Vol.105, No.GT10, pp.1233-1246.
12. Yamamuro, J. A. and Lade, P. V. (1997), "Static liquefaction of very loose sands", *Canadian Geotechnical Journal*, Vol.34, pp. 918-928.
13. Yamamuro, J. A., Covert, K. M., and Lade, P. V. (1999), "Static and cyclic liquefaction of silty sands", *Physics and Mechanics of Soil Liquefaction*, eds. Lade & Yamamuro, Balkema, Rotterdam, pp.55-65.
14. Yoshimi, Y. and Ohoka, H. (1975), "Influence of degree of shear stress reversal on the liquefaction potential of saturated sand", *Soils and Foundations*, Vol.15, No.3, pp.27-40.


(received on Apr. 20, 2002, accepted on May 27, 2002)